

Statistical Learning in Preclinical Drug Proarrhythmic Assessment

Nan Miles Xi ^{a,*}, Yu-Yi Hsu ^b, Qianyu Dang ^b, and Dalong Patrick Huang ^{b,*}

^a *Department of Mathematics and Statistics, Loyola University Chicago, Chicago, IL 60660, USA*

^b *Office of Biostatistics, Office of Translational Science, Center for Drug Evaluation and Research, US Food and Drug Administration, Silver Spring, MD 20993, USA*

* Correspondence: Nan Miles Xi (mxil@luc.edu)

Dalong Patrick Huang (Dalong.Huang@fda.hhs.gov)

Disclaimer: This paper reflects the views of the authors and should not be construed to represent FDA's views or policies

Statistical Learning in Preclinical Drug Proarrhythmic Assessment

ABSTRACT

Torsades de pointes (TdP) is an irregular heart rhythm characterized by faster beat rates and potentially could lead to sudden cardiac death. Much effort has been invested in understanding the drug-induced TdP in preclinical studies. However, a comprehensive statistical learning framework that can accurately predict the drug-induced TdP risk from preclinical data is still lacking. We proposed ordinal logistic regression and ordinal random forest models to predict low-, intermediate-, and high-risk drugs based on datasets generated from two experimental protocols. Leave-one-drug-out cross-validation, stratified bootstrap, and permutation predictor importance were applied to estimate and interpret the model performance under uncertainty. The potential outlier drugs identified by our models are consistent with their descriptions in the literature. Our method is accurate, interpretable, and thus useable as supplemental evidence in the drug safety assessment.

Keywords: statistical learning; ordinal logistic regression; ordinal random forest; drug safety assessment; prediction of torsades de pointes

Introduction

Torsades de pointes (TdP) is a rare but potentially fatal ventricular arrhythmia largely caused by electrolyte imbalance and cardiomyopathies after drug treatment.¹ TdP typically occurs with QT prolongation and results in polymorphic ventricular tachycardia.² The identification of TdP is a crucial step in the assessment of safety before a drug reaches the market.³ The International Council on Harmonisation (ICH) proposed two regulatory guidelines, ICH S7B and ICH E14, to assess the drug-induced TdP risk in preclinical and clinical studies, respectively.^{4,5} The ICH S7B

recommends using an ionic channel, hERG current, as the proxy to evaluate drug-induced TdP risk *in vitro*. Drugs blocking the hERG current are considered candidates with high TdP risk. The ICH E14 outlines a framework to examine the drug's capacity to prolong QT intervals *in vitro*. High TdP risk is assigned to drugs that induce the prolonged QT intervals in the electrocardiogram (ECG). Both guidelines focus on a single indicator of TdP risk and show high sensitivity (true positive rate) in the identification of drugs with high TdP risk. However, the overemphasis of hERG block or QT prolongation alone leads to conservative assessment and low specificity (true negative rate), potentially eliminating safe, promising drugs from the market.⁶

Previous studies revealed the factors beyond the hERG block in the assessment of drug-induced TdP risk. For example, inhibiting inward sodium or calcium currents offsets the effects of hERG block, and drugs with such mechanism show low TdP risk.⁷ Realizing the limitation of ICH S7B and ICH E14, the regulatory agency, pharmaceutical industry, and academia proposed several new paradigms to incorporate this multichannel interaction for better prediction of drug-induced TdP risk in preclinical studies. The Comprehensive *In Vitro* Proarrhythmia Assay (CiPA), initiated by the US Food and Drug Administration (FDA), is an essential public-private collaboration among these attempts.⁸ The CiPA initiative relies on the drug effects on human ventricular electrical activity measured by cellular electrophysiology of human-induced pluripotent stem cell-derived cardiomyocytes (hiPSC-CMs).⁹ It incorporates multiple ion channels beyond hERG and *in silico* modeling to predict drug-induced TdP risk. Twenty-eight drugs with clearly understood TdP risks in the market were selected as the benchmark set for the validation of the CiPA initiative. Additionally, the rabbit ventricular wedge assay (RVWA), an established *in vitro* paradigm for detecting drug-induced QT prolongation and arrhythmia,^{10,11} has been adapted for the assessment of drug-induced TdP risk.^{12,13} RVWA relies on the drug effects on the rabbit left ventricular wedge

measured by pseudo-ECG. A previous study applied RVWA to 28 CiPA drugs and exhibited promising assessment results using a normalized TdP score.¹⁴

Built on the development of *in vitro* paradigms, *in silico* models for predicting drug-induced TdP risk have been promoted in numerous studies.^{15–18} The prediction is essentially a classification problem fit into the statistical learning framework — given the input data of one drug from the *in vitro* study, the model outputs the risk of that drug. Therefore, the principles of statistical learning should be accommodated into the design of such models.¹⁹ First, the model is expected to output both classifying and ranking measurements of drug-induced TdP risk. Second, the uncertainty of such measurements is required to incorporate the variation in the experiment and modeling. Third, the model must provide an unbiased estimate of prediction performance on drugs outside the available data. Fourth, the statistical learning model itself should be able to capture both linear and nonlinear relationships in the data. Finally, the model prediction can be easily interpreted to offer mechanistic insights into the drug-induced TdP risk. Current *in silico* models mainly use score-based decision rules or simple linear regression methods. A statistical learning method satisfying the five principles is lacking.

In this study, we proposed two statistical learning models, ordinal logistic regression and ordinal random forest, to accurately predict drug-induced TdP risk on datasets generated under CiPA and RVWA paradigms. Our predictive models utilized the ordinal information in low-, intermediate-, and high-risk levels instead of treating them as independent categories. The unbiased model performance on new drugs was estimated by leave-one-drug-out cross-validation (LODO-CV). The uncertainty of model performance was further quantified by stratified bootstrap. We identified the potential outlier drugs using the asymptotic prediction accuracy obtained from stratified bootstrap. Sensitivity analysis was then conducted to investigate the impact of potential outlier

drugs on the model performance. To further validate and improve model prediction, we conducted control analysis, a common practice in *in vitro* studies, by selecting one control drug with mechanistically understood TdP risk. Finally, we examined the model interpretability through the analysis of normalized permutation predictor importance.

The proposed modeling strategies were evaluated on datasets from two recently published studies — the stem cell dataset under the CiPA paradigm and the wedge dataset under the RVWA paradigm.^{6,14} Both datasets contain the same 28 CiPA drugs with known low, intermediate, or high TdP risks ([Supplementary Table S1](#)) and multiple observations for each drug. The ordinal logistic regression and ordinal random forest exhibited similar prediction performance on the stem cell dataset in terms of four measurements. On the other hand, ordinal random forest consistently outperformed ordinal logistic regression on the wedge dataset measured by the same four measurements. The identified potential outlier drugs were consistent with the abnormal observations reported in the original studies. The model performance significantly improved after removing potential outlier drugs from the original datasets. We also found that the two models performed better conditioned on the correct prediction of the control drug. The model specification was further validated by the top predictors in terms of normalized permutation predictor importance. In summary, our work is the first attempt to construct multivariate statistical learning models that can accurately predict the drug-induced TdP risk from *in vitro* data. It satisfies the principles of statistical learning, highlighted by its comprehensive uncertainty measurements and strong interpretability. The proposed modeling and evaluation process can be extended easily to new datasets generated by other experimental protocols. The result of model prediction will serve as supplemental evidence in the drug safety assessment.

Datasets

Stem cell dataset

The first dataset was generated from a blinded *in vitro* study that aimed to assess the drug-induced TdP risk on hiPSC-CMs.⁶ The experiments in this study contain 28 drugs selected by the CiPA initiative with known low, intermediate, and high TdP risk. Electrophysiological responses of hiPSC-CMs to 28 drugs at certain concentrations were recorded, resulting in seven predictors in the dataset ([Supplementary Table S2](#)). There are two commercial human cardiomyocyte lines, five electrophysiological devices, and 10 sites involved in the experiments. For each drug, 15 observations were recorded based on the combinations of sites, cell lines, and electrophysiological devices. In total, there are 420 observations in this dataset (15 observations \times 28 drugs), and we refer to it as the stem cell dataset in the following text.

Wedge Dataset

The second dataset was generated from a blinded *in vitro* study of RVWA for the assessment of drug-induced proarrhythmia.¹⁴ The same 28 CiPA drugs were applied to RVWA, and 15 predictors were obtained from the corresponding electrophysiological responses ([Supplementary Table S3](#)). For each drug, four observations were collected in one laboratory under the same biological model and electrophysiological device. There are 112 observations in this dataset (4 observations \times 28 drugs), and we refer to it as the wedge dataset in the following text.

Methods

Missing value imputation

The stem cell and wedge datasets contain missing values due to the incomplete recording of raw electrophysiological signals in the experiments. To solve this issue, we utilized the association among predictors to impute missing values in both datasets. First, we trained a bagged tree model,²⁰ an imputation method that has shown better performance over others in previous studies,²¹ by

treating predictors with missing values as dependent variables and other predictors as independent variables. Second, we used the pretrained bagged tree model to predict the missing values through the complete predictors and observations. It is worth noting that we did not use the TdP risk information of 28 drugs in the imputation process. Therefore, the information of the prediction target, drug-induced TdP risk, did not leak to the predictors through imputation, thereby avoiding the overfitting in the model prediction. In the imputation process, we include all seven predictors in the stem cell dataset and all 15 predictors in the wedge dataset.

Model evaluation strategy

The model evaluation aims to estimate the prediction accuracy of new drugs not contained in the dataset that helped train the model. A valid evaluation strategy should generate an unbiased estimate of the model performance irrespective of the model specification. To achieve this goal, we designed an LODO-CV strategy (Figure 1).¹⁹ For each dataset in this study, we first trained a predictive model on the observations of 27 drugs and predicted the risk of observations in the one left-out drug. Then we repeated the same process by treating each drug as the left-out drug and predicting its observations by models trained on the observations of the other 27 drugs. Finally, we combined the prediction result of each drug and calculated the model performance measurement.

We take the calculation of three-category prediction accuracy as an example to illustrate the proposed LODO-CV. Let N be the number of drugs in the dataset ($N = 28$ in both datasets) and J be the number of observations per drug ($J = 15$ in the stem cell dataset; $J = 4$ in the wedge dataset). Denote \hat{f}^{-k} as the predictive model trained on the dataset *without* the observations of drug k . Let (x_j^k, y_j^k) be the j th observation of drug k , where x and y refer to the predictor vector and risk

category, respectively. Then the three-category prediction accuracy under LODO-CV, $acc_{LODO-CV}$, is calculated as:

$$acc_{LODO-CV} = \frac{1}{N} \sum_{k=1}^N \frac{1}{J} \sum_{j=1}^J I(y_j^k = \hat{f}^{-k}(x_j^k))$$

where $I(x)$ is the indicator function.

The prediction performance estimated by LODO-CV has three advantages. First, unlike previous studies that only used a small proportion of drugs in the dataset to train the model,¹⁸ LODO-CV maximizes the size of the training set, i.e., 27 drugs, and thus reduces the power loss in the validation. Second, it eliminates the model overfitting because there are no observations of the same drug in both training and test sets. Third, the prediction of left-out drugs imitates the scenario in which the model predicts a new drug beyond the existing data. It should be emphasized that LODO-CV is to provide an unbiased estimate of model performance. In the real-world application, we train the model once on all available data (e.g., 28 drugs in our study) and predict observations/drugs generated from new experiments.

Utilization of ordinal information

The prediction of drug-induced TdP risk is essentially a three-category classification problem. Given one vector of predictors (one observation) collected from experiments, the predictive model will output one of the three risk categories. Different from vanilla classification tasks, the three risk categories are not independent — ordinal information exists in the risk categories, i.e., low risk < intermediate risk < high risk. The appropriate utilization of ordinal information can improve the model prediction power.^{22,23} We utilized the ordinal information by transforming the three-category classification problem into two binary classification problems.²⁴ First, we trained a binary

classifier \hat{f}_1 which differentiated observations between low risk and intermediate-or-high risk. Similarly, we trained another binary classifier \hat{f}_2 which differentiated observations between high risk and low-or-intermediate risk. Second, for any observation x in the test set (i.e., the left-out drug), we predicted its probability of low risk $p_x(L)$, intermediate-or-high risk $p_x(MH)$, high risk $p_x(H)$, and low-or-intermediate risk $p_x(LM)$ as:

$$p_x(L) = \hat{f}_1(x),$$

$$p_x(MH) = 1 - p_x(L),$$

$$p_x(H) = \hat{f}_2(x),$$

$$p_x(LM) = 1 - p_x(H).$$

Then the probability of intermediate risk $p_x(M)$ was calculated as

$$p_x(M) = p_x(MH) - p_x(H).$$

Finally, the risk of *observation* x , $\widehat{risk}(x)$, was predicted as

$$\widehat{risk}(x) = \operatorname{argmax}_r \{p_x(r)\}$$

where $r \in \{L, M, H\}$. To predict the *drug* risk, we averaged the risk probability of observations in each drug and selected the risk category with the highest probability. Let J be the number of observations per drug and $\{x_j^k\}$ be the observations of drug k , where $j = 1, 2, \dots, J$. Given the observations' risk probabilities $\{p_{x_j^k}(L), p_{x_j^k}(M), p_{x_j^k}(H)\}$, the drug k 's probabilities of low risk $p_k(L)$, intermediate risk $p_k(M)$, and high risk $p_k(H)$ were calculated as:

$$p_k(L) = \frac{1}{J} \sum_{j=1}^J p_{x_j^k}(L)$$

$$p_k(M) = \frac{1}{J} \sum_{j=1}^J p_{x_j^k}(M)$$

$$p_k(H) = \frac{1}{J} \sum_{j=1}^J p_{x_j^k}(H)$$

Then the risk of drug k , $\widehat{risk}(k)$, was predicted as:

$$\widehat{risk}(k) = \operatorname{argmax}_r \{p_k(r)\}$$

where $r \in \{L, M, H\}$. Note that this framework can accommodate any form of binary classifiers if they can output the probability of each risk category.

Ordinal logistic regression model

The first model we built is ordinal logistic regression, in which logistic regressions were substituted for the two binary classifiers in the proposed ordinal framework. Formally, for any observation x , the two binary classifiers \hat{f}_1 and \hat{f}_2 in the ordinal framework are defined as:

$$\hat{f}_1: \log \frac{p_x(L)}{1-p_x(L)} = X\hat{\beta}_1$$

$$\hat{f}_2: \log \frac{p_x(H)}{1-p_x(H)} = X\hat{\beta}_2$$

where X is the predictor vector of observation x and $\hat{\beta}_1$ and $\hat{\beta}_2$ are two model parameter vectors (including intercepts). $X\hat{\beta}_1$ and $X\hat{\beta}_2$ are inner products between predictor vectors and parameter vectors. We estimated \hat{f}_1 and \hat{f}_2 by maximum likelihood estimation. After obtaining \hat{f}_1

and \hat{f}_2 , the prediction of risk categories for each observation and drug were calculated as described in the previous section.

Ordinal random forest model

The second model we built is ordinal random forest, in which random forests were substituted for the two binary classifiers in the proposed ordinal framework. Random forest is the ensemble of multiple decision trees and can capture the nonlinear relationship in the dataset.²⁵ A decision tree T is a predictive model that assigns each observation to a certain category based on split rules defined on the predictor space. Formally, suppose that there are P predictors X_1, X_2, \dots, X_P in the dataset, and we split the predictor space into two regions, R_1 and R_2 , according to predictor X_t and threshold s :

$$R_1(x, t, s) = \{x | X_t \leq s\}$$

$$R_2(x, t, s) = \{x | X_t > s\}$$

where x denotes observation. Then for any region R_m with N_m observations, let \hat{p}_{mr} be the proportion of category r in region R_m :

$$\hat{p}_{mr} = \frac{1}{N_m} \sum_{x_i \in R_m} I(y_i = r)$$

where x_i and y_i are the predictor vector and risk category of observation i , respectively. $I(x)$ is the indicator function. The risk of any observation x in region R_m is predicted as:

$$\widehat{risk}(x) = \operatorname{argmax}_r \hat{p}_{mr},$$

where $r \in \{L, M, H\}$. In each split generating regions R_1 and R_2 , we seek the predictor X_t and threshold s by solving the following optimization task:

$$\min_{t,s} \left[\sum_{x_i \in R_1(t,s)} L(\widehat{risk}(x_i), y_i) + \sum_{x_l \in R_2(t,s)} L(\widehat{risk}(x_l), y_l) \right]$$

where $L(x, y)$ is the loss function that can be misclassification error, Gini index, or cross-entropy.

¹⁹ The splitting process continues until it satisfies certain stopping rules, usually the maximum number of splits (tree depth) or the minimum number of observations per region (leaf size). In our implementation, we set the leaf size to 1, the default value in the R package randomForest.²⁶

To build a random forest from multiple decision trees, we generated B ($B = 500$ in our implementation) bootstrap samples from the training set. We applied the previous splitting rule to build one decision tree for each bootstrap sample. Instead of searching all P predictors, we randomly selected \sqrt{P} predictors in each split to reduce the correlation among different decision trees. The final random forest $\{T_b\}_1^B$ contains B decision trees, and the prediction of risk is the majority vote of all decision trees. As random forest is a combination of decision trees with low correlations, it reduces the high prediction variance of a single decision tree and thus exhibits high prediction accuracy in real-world applications.²⁷

Model performance measurements

We quantified the model performance by four measurements: three-category prediction accuracy, two areas under the receiver operating characteristics curve (AUROCs) (high risk vs. intermediate-or-low risk and high-or-intermediate risk vs. low risk), and concordance index. All measurements were calculated under the LODO-CV measured by both observations and drugs.

The three-category prediction accuracy is to measure the model's capacity of classifying low-, intermediate-, and high-risk observations and drugs. Suppose that there are N observations and J drugs in the dataset. Let \hat{y}_{i_obs} and y_{i_obs} be the predicted and true risks for observation i , and

\hat{y}_{j_drug} and y_{i_drug} be the predicted and true risks for drug j . The three-category prediction accuracy by observations acc_{obs} and by drug acc_{drug} were calculated as:

$$acc_{obs} = \frac{1}{N} \sum_{i=1}^N I(\hat{y}_{i_obs} = y_{i_obs})$$

$$acc_{drug} = \frac{1}{J} \sum_{j=1}^J I(\hat{y}_{j_drug} = y_{j_drug})$$

where $I(x)$ is the indicator function.

The AUROC of high risk vs. intermediate-or-low risk and AUROC of high-or-intermediate risk vs. low risk measure the model's diagnostic ability as two binary classifiers. For each observation and drug, we first calculated its probabilities of low risk $p(L)$, intermediate-or-high risk $p(MH)$, high risk $p(H)$, and low-or-intermediate risk $p(LM)$. Then we plotted the true positive rate (TPR) against the false positive rate (FPR) at various thresholds and calculated the area under that curve. The calculation of two AUROCs was implemented by R package PRROC.²⁸

The concordance index evaluates the quality of ranking in the ordinal prediction task. It was calculated as the proportion of concordant risk pairs in all predicted risk pairs by observations or drugs.²⁹ We calculated the concordance index by using R package reticulate³⁰ to call Python library lifelines.³¹

Results

Overall model performance

We used the R programming language³² to implement the proposed modeling and validation strategies. [Table 1](#) shows the prediction result of ordinal logistic regression and ordinal random

forest on the stem cell dataset. If measured by observations, the ordinal logistic regression has higher AUROC of high risk vs. intermediate-or-low risk (0.817) and concordance index (0.764). On the other hand, the ordinal random forest shows advantages in terms of the three-category prediction accuracy (0.602) and AUROC of high-or-intermediate risk vs. low risk (0.830). If measured by drugs, the ordinal logistic regression has higher three-category prediction accuracy (0.643) and concordance index (0.811), while the ordinal random forest shows advantages in terms of two AUROCs (0.900 and 0.889). Overall, the two models exhibit mixed performance on the stem cell dataset. No model consistently outperforms the other, and the gaps of different measurements between the two models range from minor to moderate. The AUROCs and concordance indices of the two models are between 0.750 and 0.850, indicating a good capacity of binary classification and order assignment. On the more difficult three-category classification task, the best prediction accuracy obtained from the same model drops to ~ 0.600 . Since the ordinal random forest can capture the nonlinear relationship,²⁵ the similar performance between the two models implies the ignorable nonlinearity in the stem cell dataset.

[Table 2](#) shows the prediction result of ordinal logistic regression and ordinal random forest on the wedge dataset. Ordinal random forest consistently outperforms ordinal logistic regression in terms of all four measurements measured by observations and drugs. The highest AUROCs and concordance indices are over 0.900, indicating excellent binary classification and order assignment. On the more difficult three-category classification task, the best prediction accuracy still exceeds 0.800. The advantage of ordinal random forest is larger measured by observations than by drugs. The superior performance of ordinal random forest over ordinal logistic regression implies the strong nonlinearity in the wedge dataset. We also note that the model performance measured by drugs is generally better than by observations on both datasets. This demonstrates the benefit of

replication in the experimental design which reduces data noise in preclinical drug proarrhythmic assessment.^{6,14,18} Interestingly, if we compare the same model across the two datasets, the model trained on the wedge dataset provides higher accuracy than on the stem cell dataset. We suspect that this is due to the experimental design of single site and platform in the wedge dataset, which likely introduces less data noise than the design of multiple sites and platforms in the stem cell dataset. However, the better model performance on the wedge dataset may overestimate the real-world prediction accuracy on other wedge datasets generated from various sites and platforms.

Model uncertainty measurement

The four measurements shown in [Table 1](#) and [Table 2](#) are point estimates of the model performance. To further understand the uncertainty of the model prediction, we conducted stratified bootstrap³³ to construct the empirical distributions of the four model performance measurements. Suppose that $Z^{(k)} = (z_1^{(k)}, z_2^{(k)}, \dots, z_J^{(k)})$ contains the observations of drug k , where $k = 1, 2, \dots, 28, J = 15$ in the stem cell dataset, and $J = 4$ in the wedge dataset. The original dataset Z is a union of $Z^{(k)}$. Let $Z^{(k)*} = (z_1^{(k)*}, z_2^{(k)*}, \dots, z_J^{(k)*})$ be a random sample of drug k drawn from $Z^{(k)}$ with replacement. The stratified bootstrap sample Z^* is constructed by the union of $Z^{(k)*}$, where $k = 1, 2, \dots, 28$. Compared with ordinary bootstrap sample, the stratified bootstrap sample preserved J repeated observations for each drug as in the original dataset Z . We generated 1000 stratified bootstrap sample Z^* s and repeated the previous model training and evaluation process on each Z^* to obtain the empirical distributions of three-category prediction accuracy, AUROC of high risk vs. intermediate-or-low risk, AUROC of high-or-intermediate risk vs. low risk, and concordance index.

Figure 2 and Table 3 compare the model uncertainty of ordinal logistic regression and ordinal random forest on the stem cell dataset. If measured by observations, the ordinal logistic regression has higher AUROC of high-or-intermediate risk vs. low risk. On the other hand, the ordinal random forest shows advantages in terms of three-category prediction accuracy and AUROC of high risk vs. intermediate-or-low risk. The concordance index is similar between the two models. If measured by drugs, the ordinal logistic regression has higher three-category prediction accuracy and concordance index, while the random forest shows advantages in terms of the two AUROCs. The two models also show comparable prediction variability. Overall, the comparison of model uncertainty on the stem cell dataset is consistent with the point estimate in Table 1 — the ordinal logistic regression and ordinal random forest exhibit similar prediction performance.

Figure 2 and Table 4 compare the uncertainty of ordinal logistic regression and ordinal random forest on the wedge dataset. Consistent with the point estimate in Table 2, ordinal random forest consistently outperforms ordinal logistic regression in terms of all four measurements. The only exception is the similar three-category prediction accuracy measured by drugs between two models. The advantage of ordinal random forest is more obvious if measured by observations than by drugs. Like the point estimate, the same model trained on the wedge dataset provides higher accuracy than on the stem cell dataset. We also note that the variability of model prediction is lower for ordinal random forest than ordinal logistic regression. Again, the high and stable performance of random forest implies strong nonlinearity in the wedge dataset.

Drug prediction analysis

We calculated the proportion of correct predictions (correct rate) for each drug in the 1000 stratified bootstrap predictions. Figure 3 shows the correct rate of predicting each drug across different model-dataset combinations. In the high-risk group, bepridil and disopyramide have

close-to-zero correct rates under both models on the stem cell dataset. However, they are better predicted in the wedge dataset, especially by the ordinal logistic regression. In the intermediate-risk group, chlorpromazine and clozapine have close-to-zero correct rates under both models in the stem cell dataset. On the other hand, cisapride and domperidone have low correct rates under both models in the wedge dataset. In the low-risk group, metoprolol and ranolazine have close-to-zero correct rates under both models in the stem cell dataset, while all drugs are predicted relatively well in the wedge dataset, except for ranolazine by the ordinal random forest.

Figure 3 also demonstrates the different asymptotic drug predictions on the two datasets. In the stem cell dataset, there are eight drugs on which both models resulted in less than 25% correct rates. These drugs with low prediction accuracy cover all three risk categories. In the wedge dataset, however, only two drugs of intermediate risk are difficult for both models to predict. If compared by models, ordinal logistic regression predicted nine drugs in the stem cell dataset and two drugs in the wedge dataset less than 25% correctly. On the other hand, ordinal random forest predicted 10 drugs in the stem cell dataset and five drugs in the wedge dataset less than 25% correctly. Although ordinal random forest shows better performance on the wedge dataset and similar performance on the stem cell dataset (Table 1-4; Figure 2), it made more “absolute wrong predictions” asymptotically. The better performance of ordinal random forest measured by the previous four measurements is largely due to its capacity of predicting more drugs with high correct rates.

Many of the drugs with close-to-zero correct rates have been reported to have abnormal observations in their original experiments.^{6,14} In the experiment of the stem cell dataset, for example, the high-risk drug bepridil surprisingly introduced no arrhythmias, a key indicator of high TdP risk, in hiPSC-CMs even at 30-fold C_{max}. Another high-risk drug, disopyramide, was

reported as being poorly soluble at the required concentrations, potentially biasing the prediction result. The two low-risk drugs with low correct rates, metoprolol and ranolazine, introduced abnormally strong signals of high TdP risk in hiPSC-CMs, including significant repolarization prolongation and arrhythmias. In the experiment of the wedge dataset, the intermediate-risk drug domperidone produced statistically significant QT prolongation at Cmax, one indicator of high TdP risk. Such observations imply that the wrong model predictions are possibly caused by an abnormality in the experiments rather than model incompetency.

Sensitivity analysis

We define the drugs with a correct rate of less than 25% under both models as potential outlier drugs. Based on the drug prediction analysis shown in [Figure 3](#), we identified eight and two potential outlier drugs in the stem cell dataset and wedge dataset, respectively. [Table 5](#) shows those drugs and their average correct rates across the two models. To examine the effects of potential outlier drugs on the model performance, we removed them from the original datasets and redid the previous modeling and validation. [Figure 4](#) compares the model performance before and after removing potential outlier drugs. First, we find that all four measurements — three-category prediction accuracy, AUROC of high risk vs. intermediate-or-low risk, AUROC of high-or-intermediate risk vs. low risk, and concordance index, improve without potential outlier drugs in the dataset, regardless of model, measured by observations or drugs, or dataset. Second, the benefit of removal is stronger in the stem cell dataset, partly because the baseline performance is already high in the wedge dataset. Third, the ordinal logistic regression and ordinal random forest have a similar performance boost after removing potential outlier drugs. Fourth, the absolute values of four measurements without potential outlier drugs are high, with many of them greater than 0.900, indicating excellent model predictive capacity. Overall, the existence of potential outlier drugs has

significant impacts on the model performance, and most wrong predictions are caused by such drugs.

Control analysis

Motivated by the practice in the experimental assessment of drug-induced TdP risk,^{34,35} we conducted control analysis to further validate the model prediction performance. Control drugs have clearly understood TdP risk; in the control analysis, the model trained on the training drugs will predict the test drug and control drug simultaneously. The predictive model is expected to correctly identify the risk of the control drug based on the data generated from the experiment. If the model prediction of the control drug is incorrect, then its simultaneous prediction on the test drug would be considered unreliable. We trust the model and its prediction of the test drug only if it can correctly predict the control drug. We select the high-risk drug sotalol as an example control drug in our analysis because of the thorough exploration of its mechanism in the literature³⁶ and its high correct rate in our drug prediction analysis (Figure 3). Any other drugs with definite TdP risk and high prediction accuracy can also be selected as the control drug.

Figure 5 shows the design of the control analysis. As with previous analyses, we trained ordinal logistic regression and ordinal random forest on the stem cell dataset and wedge dataset and validated the model performance using LODO-CV. In each step, the model was trained on a set with 26 drugs and predicted the risk of one left-out test drug and one pre-selected control drug (sotalol) simultaneously. The four model performance measurements were calculated for each test drug, conditioned on the correct prediction of control drug (with control) and no condition (without control). All measurements were calculated by observations and drugs. Table 6 compares the model performance with and without control across all model-dataset combinations. Among the 16 measurements in the stem cell dataset, most of them with control are higher than (13) or equal

to (2) their counterparts without control, except for the AUROC of high-or-intermediate risk vs. low risk under ordinal random forest by drugs. Among the eight measurements of ordinal logistic regression in the wedge dataset, most of them are higher than (6) or equal to (1) their counterparts without control, except for the AUROC of high-or-intermediate risk vs. low risk by observations. Ordinal random forest has the same performance regardless of control because the prediction accuracy of the control drug is 100%. The result of control analysis illustrates that the prediction of a control drug is an effective indicator of model capacity — the models that can correctly predict control drugs generally perform better than those that cannot. In practice, we may consider the model outputs conditioned on the correct prediction of the control drug as high-confidence results and other outputs as low-confidence results. It should be noted that there must be appropriate control drugs in the original dataset to conduct the control analysis.

Predictor importance analysis

To examine the effect of various predictors on the model performance, we conducted a predictor importance analysis. We utilized the permutation prediction importance^{25,37} to measure the contribution of each predictor to the model prediction. The permutation predictor importance of one predictor is defined as the decrease of the model prediction accuracy when that predictor's value is randomly shuffled. Since the random shuffling breaks the relationship between the predictor and target variable (TdP risk), the decrease of the prediction accuracy (if any) indicates the model dependency on that shuffled predictor. Using permutation predictor importance has three advantages. First, the calculation of permutation predictor importance is independent of the specific model form. Second, the predictive model only needs to be trained once. Third, the random shuffling can be repeated multiple times to reduce the variability in the calculation.

Suppose there are P predictors in dataset D , and \hat{f} is a pretrained predictive model. Let acc be the upper bound of 95% confidence interval of three-category prediction accuracy measured by observations (Table 3 and Table 4). For each predictor j (j th column of D) and each repetition g in $1, \dots, G$, we perform the following calculations:

1. Randomly shuffle the j th column of dataset D to generate a permuted dataset $\widetilde{D}_{g,j}$
2. Calculate the three-category prediction accuracy $acc_{g,j}$ on the permuted dataset $\widetilde{D}_{g,j}$

Then the permutation importance of predictor j , imp_j , is calculated as

$$imp_j = acc - \frac{1}{G} \sum_{g=1}^G acc_{g,j}$$

Finally, we calculate the normalized permutation predictor importance of predictor j , $nimp_j$, by

$$nimp_j = \frac{imp_j}{\max \{imp_1, imp_2, \dots, imp_j\}}$$

In our implementation, we set the repetition number G to 100 and \hat{f} to ordinal random forest.

Figure 6 shows the normalized permutation predictor importance for all seven predictors in the stem cell dataset and top-seven predictors in the wedge dataset. In the stem cell dataset, the top-two important predictors in terms of contribution to prediction accuracy are 1) the drug concentration when drug-induced arrhythmias were first observed (foldaym); 2) whether drug-induced arrhythmias occurred at any concentration in more than 40% wells (AMtwooutoffive). These two predictors also lead to a large margin of importance over other predictors. This result is consistent with the previous study showing that the introduction of arrhythmias is the most important factor in the identification of drug-induced TdP risk on the hiPSC-CMs protocol.^{9,38}

In the wedge dataset, the top-two important predictors are 1) interval between the J point and the start of T wave (c3v2); 2) interval between the J point and the peak of T wave (c3v3). They also echo the previous findings in the experiments of RVWA.^{11,12} The consistency between model discovery and established drug-risk mechanism further validates the model specification and provides another insight into the model interpretability. It should be mentioned that the permutation predictor importance emphasizes the marginal effects of predictors on the model prediction.³⁹ Therefore, the non-top important predictors in [Figure 6](#) may also impact the model performance through their interactions with other predictors.

Discussion

The overall model performance, uncertainty measurement, and drug prediction demonstrate that the prediction accuracy of two models on the wedge dataset is consistently higher than the stem cell dataset. Such discrepancy is largely due to the different experimental designs of the two datasets. Observations in the stem cell dataset were generated at 10 experimental sites, using two hiPSC-CM lines and five EP platforms. On the other hand, all observations in the wedge dataset were generated at one laboratory using the same type of biological sample and EP platform. Although the multisite experiments were supposed to follow the same protocols, the batch effects caused by site-to-site variability introduced a higher degree of noise in the stem cell dataset. The signal-noise ratio in the stem cell dataset is thus lower than the wedge dataset, resulting in lower prediction accuracy. One potential solution for this issue is to estimate the effects of site, cell line, and EP platform and include these factors into the modeling process. The accurate estimation of such effects requires special experimental designs with enough power to describe and explain the variations from those factors.⁴⁰⁻⁴³

Besides the CiPA and RVWA paradigms, there are many *in vitro* protocols aiming to assess the drug-induced TdP risk, including automated patch clamp,⁴⁴ human ventricular myocyte model,¹⁵ rabbit isolated hearts,⁴⁵ *in vitro* atrioventricular block dog,¹⁶ and others. It is difficult to fairly compare those protocols because they were developed under various biological models, experimental conditions, methods of data collection, and predictor formulation. One future work is to utilize our statistical learning framework to examine the power of these protocols in the assessment of drug-induced TdP risk. A statistical learning model, e.g., an ordinal random forest, can be trained on datasets generated by different protocols. The comparison of model performance across different datasets will serve as a proxy of the protocol's strength. Another future direction is to encompass novel experimental techniques and measurements beyond electrophysiological signals into the *in vitro* paradigm. For example, single-cell RNA-sequencing (scRNA-seq),⁴⁶ a next-generation sequencing technology revealing the genome-wide gene expression at single-cell levels, can be applied to evaluate and compare the transcriptomes of individual cells before and after drug treatment.⁴⁷⁻⁴⁹ The gene expression dynamic associated with drug-induced TdP risk will potentially improve the assessment of such risks, similar to the progress made by scRNA-seq in cancer diagnosis, cell type discovery, and precision medicine.^{50,51}

In summary, we proposed a comprehensive statistical modeling framework to predict drug-induced TdP risk from two preclinical experimental protocols. Ordinal logistic regression and ordinal random forest were trained on the stem cell dataset and wedge dataset. We calculated the unbiased estimate of model performance by LODO-CV. The uncertainty of model performance was evaluated by stratified bootstrap. Our proposed method provided interpretability consistent with domain knowledge through normalized permutation prediction importance. Sensitivity analysis identified potential outlier drugs that were also described in the literature. Finally, we

conducted a control analysis and further validated the model performance. Our work is a valuable addition to the current attempts to construct trustful *in silico* models in the assessment of drug-induced TdP risk.

Acknowledgments

We thank Dr. Gan-Xin Yan for sharing the wedge dataset with us. We also thank the Health and Environmental Sciences Institute (HESI) for providing the stem cell dataset from the hiPSC-CMs study funded by FDA Broad Agency Announcement (BAA) contract (FDABAA-15-00121). We are grateful for the valuable discussions with Drs. Christine Garnett, Donglin Guo, Lars Johannesen, Jose Vicente Ruiz, and Wendy Wu. Finally, we want to thank Drs. Yi Tsong and Atiar Rahman for their support for this project.

References

1. Al-Khatib, S. M., Stevenson, W.G., Ackerman, M. J., et al. 2018. 2017 AHA/ACC/HRS guideline for management of patients with ventricular arrhythmias and the prevention of sudden cardiac death: Executive summary: A report of the American college of cardiology/American heart association task force on clinical practice guidelines and the heart rhythm society. *Journal of the American College of Cardiology* **72**, 1677–1749.
2. Joshi, A., Dimino, T., Vohra, Y., Cui, C. & Yan, G.-X. 2004. Preclinical strategies to assess QT liability and torsadogenic potential of new drugs: the role of experimental models. *Journal of Electrocardiology* **37** Suppl, 7–14.
3. Stockbridge, N., Morganroth, J., Shah, R. R. & Garnett, C. 2013. Dealing with global safety issues : was the response to QT-liability of non-cardiac drugs well coordinated? *Drug Safety* **36**, 167–182.
4. Cavero, I. & Crumb, W. 2005. ICH S7B draft guideline on the non-clinical strategy for testing delayed cardiac repolarisation risk of drugs: a critical analysis. *Expert Opinion on Drug Safety* **4**, 509–530.
5. Shah, R. R. 2005. Drugs, QTc interval prolongation and final ICH E14 guideline: an important milestone with challenges ahead. *Drug Safety* **28** 1009–1028.
6. Blinova, K. et al. International multisite study of human-induced pluripotent stem cell-derived cardiomyocytes for drug proarrhythmic potential assessment. *Cell Reports* **24**, 3582–3592 (2018).
7. Badri, M. et al. Mexiletine prevents recurrent torsades de pointes in acquired long QT syndrome refractory to conventional measures. *JACC Clinical Electrophysiology* **1**, 315–322 (2015).
8. Fermini, B. et al. 2016. A new perspective in the field of cardiac safety testing through the comprehensive in vitro proarrhythmia assay paradigm. *Journal of Biomolecular Screening* **21**, 1–11.

9. Vicente, J. et al. 2018. Mechanistic model-informed proarrhythmic risk assessment of drugs: Review of the “CiPA” initiative and design of a prospective clinical validation study. *Clinical Pharmacology & Therapeutics* **103**, 54–66.
10. Yan, G. X. et al. 2001. Ventricular hypertrophy amplifies transmural repolarization dispersion and induces early afterdepolarization. *American Journal of Physiology Heart and Circulatory Physiology* **281**, H1968-75.
11. Wang, D., Patel, C., Cui, C. & Yan, G.-X. 2008. Preclinical assessment of drug-induced proarrhythmias: role of the arterially perfused rabbit left ventricular wedge preparation. *Pharmacology & Therapeutics* **119**, 141–151.
12. Liu, T., Brown, B.S., Wu, Y., Antzelevitch, C., Kowey, P.R. & Yan, G.-X. 2006. Blinded validation of the isolated arterially perfused rabbit ventricular wedge in preclinical assessment of drug-induced proarrhythmias. *Heart Rhythm* **3**, 948–956.
13. Liu, T. et al. 2013. Differentiating electrophysiological effects and cardiac safety of drugs based on in vitro electrocardiogram: A blinded validation. *Journal of Pharmacological and Toxicological Methods* **68**, e23.
14. Liu, T. et al. 2021. Utility of Normalized TdP Score System in drug proarrhythmic potential assessment: A blinded in vitro study of CiPA drugs. *Clinical Pharmacology & Therapeutics* **109**, 1606–1617.
15. Lancaster, M. C. & Sobie, E. A. 2016. Improved Prediction of Drug-Induced Torsades de Pointes Through Simulations of Dynamics and Machine Learning Algorithms. *Clinical Pharmacology & Therapeutics* **100**, 371–379.
16. Passini, E. et al. 2017. Human in silico drug trials demonstrate higher accuracy than animal models in predicting clinical pro-arrhythmic cardiotoxicity. *Frontiers in Physiology* **8**: 668.
17. Okada, J.-I. et al. 2015. Screening system for drug-induced arrhythmogenic risk combining a patch clamp and heart simulator. *Science Advances* **1**, e1400142.
18. Li, Z. et al. 2019. Assessment of an in silico mechanistic model for proarrhythmia risk prediction under the CiPA initiative. *Clinical Pharmacology & Therapeutics* **105**, 466–475.
19. Hastie, T., Tibshirani, R. & Friedman, J. 2009. *The Elements of Statistical Learning: Data Mining, Inference, and Prediction, Second Edition*. 2nd ed. New York: Springer Science & Business Media.
20. Breiman, L. 1996. Bagging predictors. *Machine Learning* **24**, 123–140.
21. Kuhn, M. 2008. Building Predictive Models in R Using the caret Package. *Journal of Statistical Software, Articles* **28**, 1–26.
22. Cardoso, J. S. & Sousa, R. 2011. Measuring the performance of ordinal classification. *International Journal of Pattern Recognition and Artificial Intelligence* **25**, 1173–1195.
23. Gaudette, L. & Japkowicz, N. 2009. Evaluation Methods for Ordinal Classification. in *Advances in Artificial Intelligence* 207–210.
24. Frank, E. & Hall, M. 2001. A Simple Approach to Ordinal Classification. in *Machine Learning: ECML 2001* 145–156.
25. Breiman, L. Random Forests. *Machine Learning* **45**, 5–32 (2001).
26. Liaw, A., Wiener, M. Classification and regression by randomForest. *R news* **2**, 18–22 (2002).
27. Couronné, R., Probst, P. & Boulesteix, A.-L. Random forest versus logistic regression: a large-scale benchmark experiment. *BMC Bioinformatics* **19**, (2018).
28. Grau, J., Grosse, I. & Keilwagen, J. 2015. PRROC: computing and visualizing precision-recall and receiver operating characteristic curves in R. *Bioinformatics* **31**, 2595–2597.

29. Raykar, V. C., Steck, H., Krishnapuram, B., Dehing-Oberije, C. & Lambin, P. 2007. On ranking in survival analysis: bounds on the concordance index. in *Proceedings of the 20th International Conference on Neural Information Processing Systems* 1209–1216 (Curran Associates Inc., 2007).
30. Allaire, J. J. *et al.* reticulate: Interface to 'Python'. *R package version 1*, (2018).
31. Davidson-Pilon, C. 2019. lifelines: survival analysis in Python. *Journal of Open Source Software***4**, 1317.
32. R Core Team 2013. R: A language and environment for statistical computing. *R Foundation for statistical computing, Vienna*.
33. Mashreghi, Z., Haziza, D. & Léger, C. 2016. A survey of bootstrap methods in finite population sampling. *Statistics Surveys*, **10**, 1–52.
34. Gintant, G. 2011. An evaluation of hERG current assay performance: Translating preclinical safety studies to clinical QT prolongation. *Pharmacology & Therapeutics* **129**, 109–119 .
35. Rampe, D. & Brown, A. M. 2013. A history of the role of the hERG channel in cardiac risk assessment. *Journal of Pharmacological and Toxicological Methods* **68**, 13–22 .
36. Singh, B. N., Kehoe, R., Woosley, R. L., Scheinman, M. & Quart, B. 1995. Multicenter trial of sotalol compared with procainamide in the suppression of inducible ventricular tachycardia: A double-blind, randomized parallel evaluation. *American Heart Journal* **129**, 87–97.
37. Altmann, A., Toloşi, L., Sander, O. & Lengauer, T. 2010. Permutation importance: a corrected feature importance measure. *Bioinformatics* **26**, 1340–1347.
38. Colatsky, T. *et al.* 2016. The Comprehensive in Vitro Proarrhythmia Assay (CiPA) initiative - Update on progress. *Journal of Pharmacological and Toxicological Methods***81**, 15–20.
39. Strobl, C., Boulesteix, A.-L., Kneib, T., Augustin, T. & Zeileis, A. 2008. Conditional variable importance for random forests. *BMC Bioinformatics* **9**, 307.
40. Wang, L., Xiao, Q. & Xu, H. 2018. Optimal maximin L_1 -distance Latin hypercube designs based on good lattice point designs. *Annals of Statistics* **46** (6B), 3741-3766.
41. Xiao, Q., Wang, L. & Xu, H. 2019. Application of kriging models for a drug combination experiment on lung cancer. *Statistics in Medicine*. **38**, 236–246.
42. Wang, L., Yang, J.-F., Lin, D. K. J. & Liu, M.-Q. Nearly Orthogonal Latin Hypercube Designs For Many Design Columns. *Statistica Sinica* **25**, 1599–1612 (2015).
43. Wang, L., Sun, F., Lin, D. K. J. & Liu, M.-Q. 2018. CONSTRUCTION OF ORTHOGONAL SYMMETRIC LATIN HYPERCUBE DESIGNS. *Statistica Sinica* **28**, 1503–1520.
44. Kramer, J. *et al.* 2013. MICE Models: Superior to the HERG Model in Predicting Torsade de Pointes. *Scientific Reprts* **3**, 1–7 (2013).
45. Vargas, H. M. *et al.* 2015. Evaluation of drug-induced QT interval prolongation in animal and human studies: a literature review of concordance. *British Journal of Pharmacology* **172**, 4002–4011 (2015).
46. Hwang, B., Lee, J. H. & Bang, D. 2018. Single-cell RNA sequencing technologies and bioinformatics pipelines. *Experimental & Molecular Medicine* **50**, 96.
47. Haque, A., Engel, J., Teichmann, S. A. & Lönnberg, T. 2017. A practical guide to single-cell RNA-sequencing for biomedical research and clinical applications. *Genome Medicine*. **9**.
48. Xi, N. M. & Li, J. J. 2021. Benchmarking Computational Doublet-Detection Methods for Single-Cell RNA Sequencing Data. *Cell Systems* **12**, 176-194.e6.
49. Xi, N. M. & Li, J. J. 2021. Protocol for executing and benchmarking eight computational doublet-detection methods in single-cell RNA sequencing data analysis. *STAR Protocols* **2**(3):100699.

50. Sun, G. *et al.* 2021. Single-cell RNA sequencing in cancer: Applications, advances, and emerging challenges. *Molecular Therapy - Oncolytics* **21**, 183–206.
51. Wiedmeier, J. E., Noel, P., Lin, W., Von Hoff, D. D. & Han, H. 2019. Single-Cell Sequencing in Precision Medicine. *Cancer Treatment and Research Communications* **178**, 237–252.
52. Christophe, B. 2015. In silico study of transmural dispersion of repolarization in non-failing human ventricular myocytes: Contribution to cardiac safety pharmacology. *British Journal of Pharmacology*. **7**, 88–101.

Figures

	Train (27 drugs)									Test
Step 1	1	2	3	4	25	26	27		28
Step 2	1	2	3	4	25	26	28		27
Step 3	1	2	3	4	25	27	28		26
⋮					⋮					
Step 27	1	3	4	5	26	27	28		2
Step 28	2	3	4	5	26	27	28		1

Measurement of model performance on 28 drugs

Figure 1. The schematic diagram of leave-one-drug-out cross-validation. In each iteration, we trained the predictive model on 27 training drugs and predicted one left-out drug. The same process was repeated until each drug was predicted, and the model performance was calculated by combining the prediction results of each left-out drug.

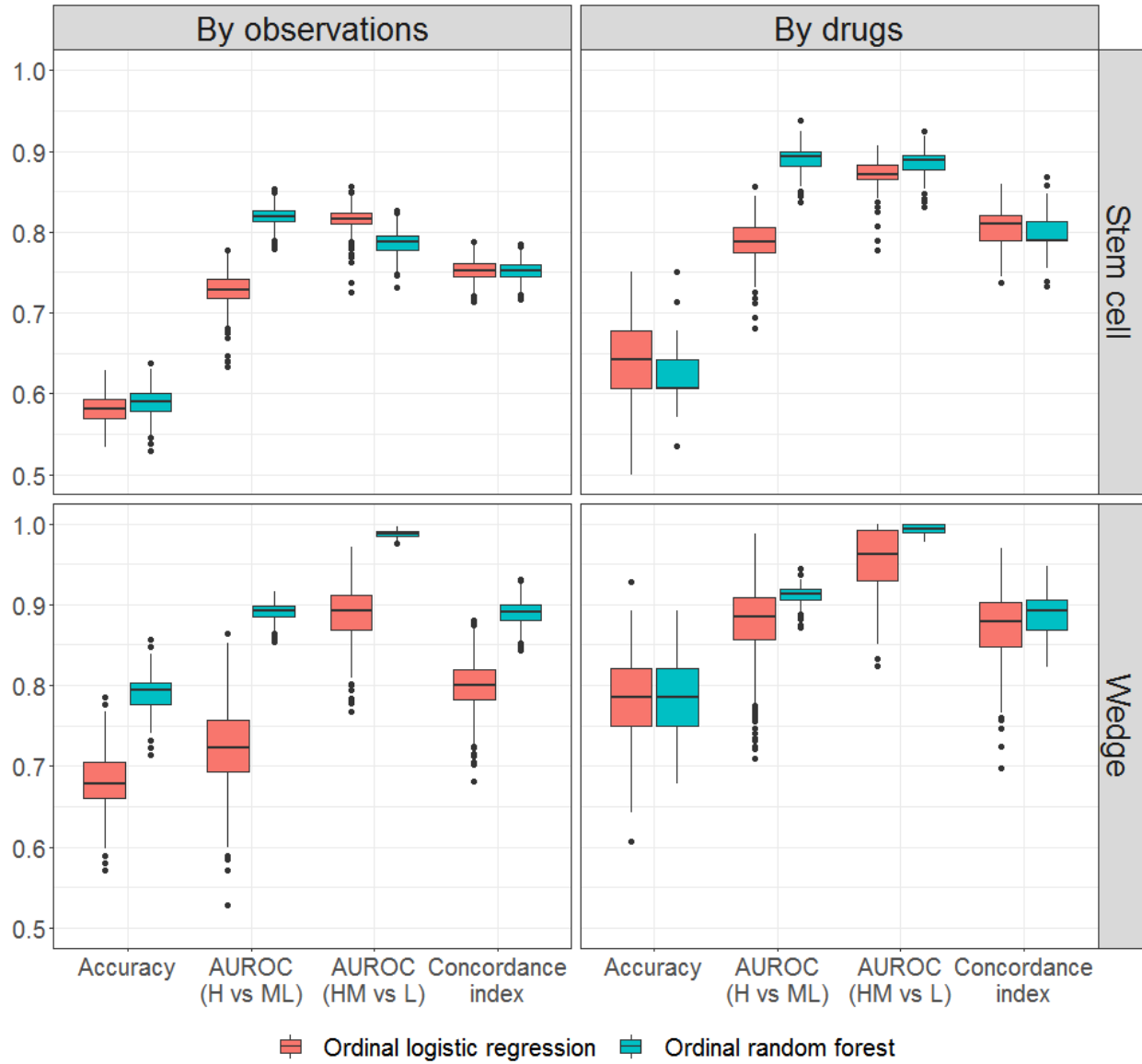


Figure 2. The empirical distributions of model performance under stratified bootstrap. Four performance measurements of two models were calculated under four conditions: 1) by observations on the stem cell dataset; 2) by drugs on the stem cell dataset; 3) by observations on the wedge dataset; 4) by drugs on the wedge dataset.

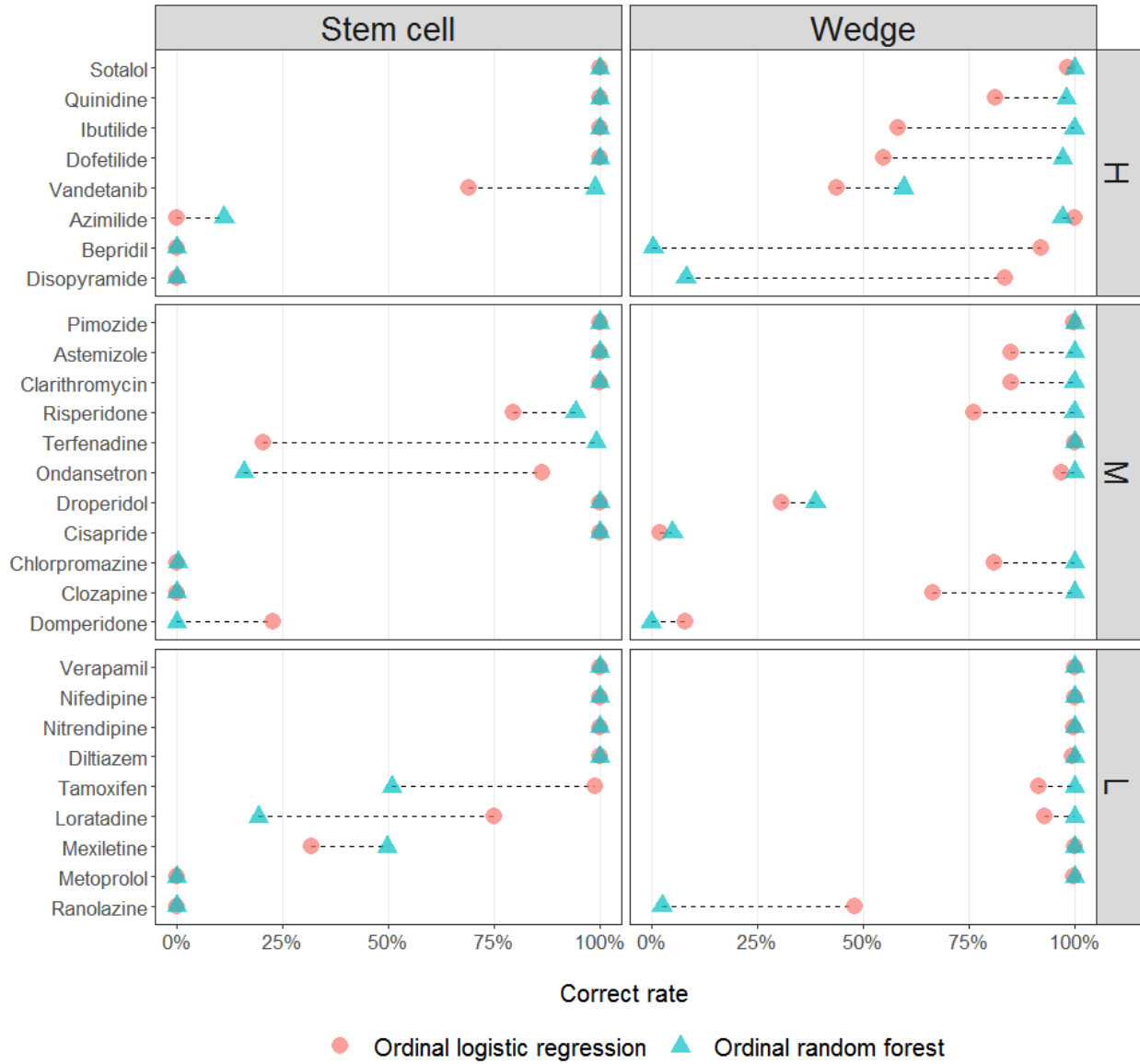


Figure 3. The correct rate of drug prediction calculated by stratified bootstrap. For each drug, we connect the correct rates of two models. In each risk category, drugs are sorted from high to low based on their average correct rates across two models.

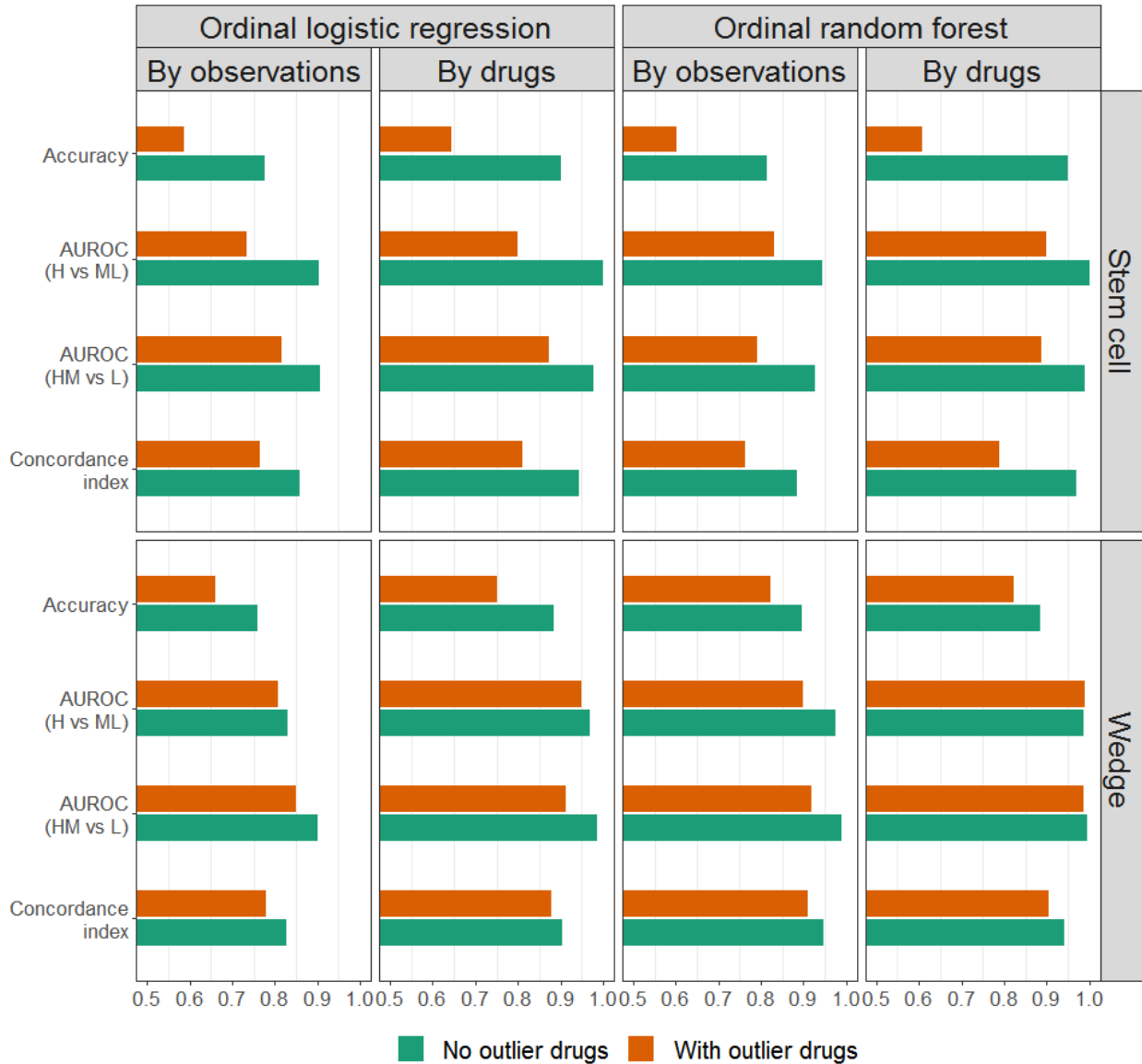


Figure 4. The model performance before and after the removal of potential outlier drugs. The four measurements were calculated under eight conditions: 1) ordinal logistic regression by observations on the stem cell dataset; 2) ordinal logistic regression by drugs on the stem cell dataset; 3) ordinal logistic regression by observations on the wedge dataset; 4) ordinal logistic regression by drugs on the wedge dataset; 5) ordinal random forest by observations on the stem cell dataset; 6) ordinal random forest by drugs on the stem cell dataset; 7) ordinal random forest by observations on the wedge dataset; 8) ordinal random forest by drugs on the wedge dataset.

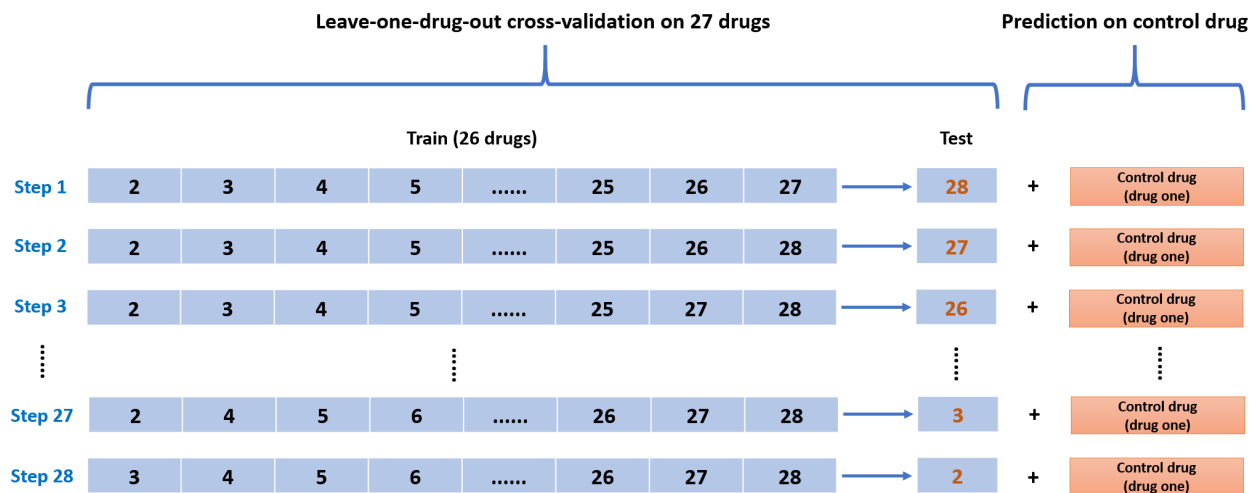


Figure 5. The schematic diagram of control analysis where drug one is the example control drug. We trained the model on 26 drugs and predicted one test drug and one control drug simultaneously. Leave-one-drug-out cross-validation was used to estimate the prediction accuracy of 27 non-control drugs and one control drug.

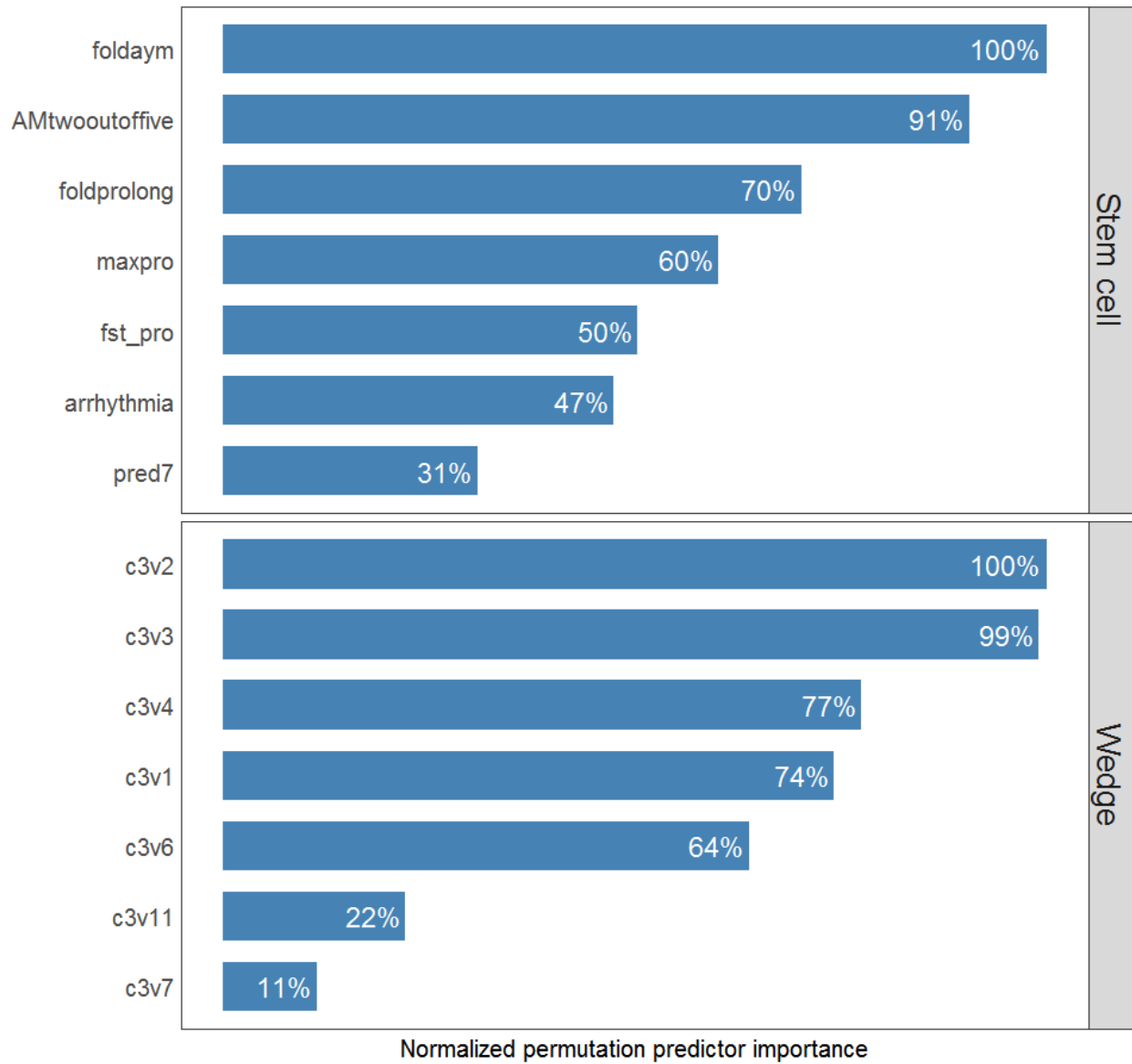


Figure 6. The normalized permutation predictor importance on the stem cell dataset and wedge dataset. Predictors are sorted from high to low. There are seven predictors in the stem cell dataset and the top-seven predictors in the wedge dataset.

Tables

Measured by	Model	Accuracy (Three-category)	AUROC (High vs. Intermediate-or-Low)	AUROC (High-or-Intermediate vs. Low)	Concordance index (Three-category)
Observations	Ordinal logistic regression	0.588	0.734	<u>0.817</u>	<u>0.764</u>
	Ordinal random forest	<u>0.602</u>	<u>0.830</u>	0.791	0.762
Drugs	Ordinal logistic regression	<u>0.643</u>	0.800	0.872	<u>0.811</u>
	Ordinal random forest	0.607	<u>0.900</u>	<u>0.889</u>	0.790

Table 1. The model performance on the stem cell dataset (point estimate). Three-category prediction accuracy, two AUROCs, and concordance index are shown for ordinal logistic regression and ordinal random forest, measured by observations and drugs, respectively. The higher values between the two models are underscored.

Measured by	Model	Accuracy (Three-category)	AUROC (High vs. Intermediate-or-Low)	AUROC (High-or-Intermediate vs. Low)	Concordance index (Three-category)
Observations	Ordinal logistic regression	0.661	0.808	0.849	0.780
	Ordinal random forest	<u>0.822</u>	<u>0.900</u>	<u>0.919</u>	<u>0.909</u>
Drugs	Ordinal logistic regression	0.750	0.950	0.913	0.879
	Ordinal random forest	<u>0.822</u>	<u>0.989</u>	<u>0.988</u>	<u>0.906</u>

Table 2. The model performance on the wedge dataset (point estimate). Three-category prediction accuracy, two AUROCs, and concordance index are shown for ordinal logistic regression and ordinal random forest, measured by observations and drugs, respectively. The higher values between the two models are underscored.

Measured by	Model	Measurement	Accuracy (Three-category)	AUROC (High vs. Intermediate-or-Low)	AUROC (High-or-Intermediate vs. Low)	Concordance index (Three-category)
Observations	Ordinal logistic regression	95% CI	(0.548, 0.615)	(0.691, 0.764)	(0.793, 0.837)	(0.730, 0.775)
		Mean	0.581	0.729	0.817	<u>0.753</u>
	Ordinal random forest	95% CI	(0.560, 0.619)	(0.799, 0.841)	(0.761, 0.813)	(0.731, 0.774)
		Mean	<u>0.590</u>	<u>0.820</u>	<u>0.787</u>	<u>0.753</u>
Drugs	Ordinal logistic regression	95% CI	(0.572, 0.715)	(0.750, 0.825)	(0.842, 0.901)	(0.763, 0.848)
		Mean	<u>0.637</u>	<u>0.789</u>	0.873	<u>0.807</u>
	Ordinal random forest	95% CI	(0.571, 0.679)	(0.857, 0.919)	(0.854, 0.913)	(0.767, 0.836)
		Mean	0.622	0.892	<u>0.885</u>	0.797

Table 3. The summary statistics of model performance under stratified bootstrap on the stem cell dataset. The 95% confidence intervals and means of four measurements were calculated for ordinal logistic regression and ordinal random forest. The higher mean values between the two models are underscored.

Measured by	Model	Measurement	Accuracy (Three-category)	AUROC (High vs. Intermediate-or-Low)	AUROC (High-or-Intermediate vs. Low)	Concordance index (Three-category)
Observations	Ordinal logistic regression	95% CI	(0.608, 0.759)	(0.628, 0.815)	(0.828, 0.949)	(0.743, 0.853)
		Mean	0.683	0.725	0.890	0.800
	Ordinal random forest	95% CI	(0.741, 0.831)	(0.870, 0.911)	(0.981, 0.995)	(0.862, 0.917)
		Mean	<u>0.790</u>	<u>0.892</u>	<u>0.988</u>	<u>0.891</u>
Drugs	Ordinal logistic regression	95% CI	(0.679, 0.893)	(0.779, 0.957)	(0.883, 1.000)	(0.784, 0.948)
		Mean	0.777	0.880	0.959	0.875
	Ordinal random forest	95% CI	(0.750, 0.858)	(0.888, 0.932)	(0.983, 1.000)	(0.860, 0.927)
		Mean	<u>0.789</u>	<u>0.913</u>	<u>0.994</u>	<u>0.890</u>

Table 4. The summary statistics of model performance under stratified bootstrap on the wedge dataset. The 95% confidence intervals and means of four measurements were calculated for ordinal logistic regression and ordinal random forest. The higher mean values between the two models are underscored.

Dataset	Drug	Average correct rate	TdP risk
Stem cell	Azimilide	0.056	High
	Bepidil	0.000	High
	Disopyramide	0.000	High
	Domperidone	0.114	Intermediate
	Chlorpromazine	0.002	Intermediate
	Clozapine	0.000	Intermediate
	Ranolazine	0.000	Low
	Metoprolol	0.000	Low
Wedge	Domperidone	0.040	Intermediate
	Cisapride	0.035	Low

Table 5. The potential outlier drugs in the stem cell dataset and wedge dataset. The potential outlier drugs are defined as drugs with both correct rates under two models less than 25%. The average correct rate is calculated by averaging the correct rates across two models.

Dataset	Measured by	Model	Measurement	Without control	With control
Stem cell	Observations	Ordinal logistic regression	Accuracy	0.587	<u>0.630</u>
			Concordance index	0.750	<u>0.780</u>
			AUROC (H vs. ML)	0.689	<u>0.732</u>
			AUROC (HM vs. L)	0.780	<u>0.826</u>
		Ordinal random forest	Accuracy	0.560	<u>0.572</u>
			Concordance index	0.723	<u>0.731</u>
			AUROC (H vs. ML)	0.797	<u>0.830</u>
			AUROC (HM vs. L)	0.774	<u>0.778</u>
	Drugs	Ordinal logistic regression	Accuracy	<u>0.629</u>	<u>0.629</u>
			Concordance index	0.782	<u>0.785</u>
			AUROC (H vs. ML)	0.750	<u>0.765</u>
			AUROC (HM vs. L)	0.833	<u>0.858</u>
		Ordinal random forest	Accuracy	0.592	<u>0.630</u>
			Concordance index	0.755	<u>0.783</u>
			AUROC (H vs. ML)	<u>0.893</u>	<u>0.893</u>
			AUROC (HM vs. L)	<u>0.882</u>	0.877
Wedge	Observations	Ordinal logistic regression	Accuracy	0.657	<u>0.670</u>
			Concordance index	0.778	<u>0.785</u>
			AUROC (H vs. ML)	0.741	<u>0.797</u>
			AUROC (HM vs. L)	<u>0.896</u>	0.895
		Ordinal random forest	Accuracy	<u>0.824</u>	<u>0.824</u>
			Concordance index	<u>0.911</u>	<u>0.911</u>
			AUROC (H vs. ML)	<u>0.895</u>	<u>0.895</u>
			AUROC (HM vs. L)	<u>0.988</u>	<u>0.988</u>
	Drugs	Ordinal logistic regression	Accuracy	0.777	<u>0.815</u>
			Concordance index	0.887	<u>0.910</u>
			AUROC (H vs. ML)	0.907	<u>0.929</u>
			AUROC (HM vs. L)	<u>0.963</u>	<u>0.963</u>
		Ordinal random forest	Accuracy	<u>0.815</u>	<u>0.815</u>
			Concordance index	<u>0.902</u>	<u>0.902</u>
			AUROC (H vs. ML)	<u>0.914</u>	<u>0.914</u>
			AUROC (HM vs. L)	<u>0.994</u>	<u>0.994</u>

Table 6. The control analysis on the stem cell dataset and wedge dataset. Sotalol was selected as the example control drug in both datasets. The higher values between with and without control are underscored.

Supplementary

Low TdP Risk (9)	Intermediate TdP Risk (11)	High TdP Risk (8)
Diltiazem, Loratadine Ranolazine, Metoprolol Mexiletine, Nifedipine Nitrendipine, Tamoxifen Verapamil	Astemizole, Chlorpromazine Cisapride, Clarithromycin Clozapine, Domperidone, Droperidol, Ondansetron, Pimozide, Risperidone, Terfenadine	Azimilide, Bepridil Disopyramide, Dofetilide Ibutilide, Quinidine Sotalol, Vandetanib

Table S1. The 28 CiPA drugs in the stem cell dataset and wedge dataset.

Predictor	Description	Type
arrhythmia	Whether drug-induced arrhythmias occurred at any concentration in any wells	Binary
AMtwooutoffive	Whether drug-induced arrhythmias occurred at any concentration in more than 40% of wells	Binary
maxpro	Maximum repolarization change (ms) observed at any concentration	Continuous
fst_pro	Repolarization prolongation (ms) at the first drug concentration with statistically significant prolongation or shortening	Continuous
foldprolong	Drug concentration (folds over C _{max}) at which the statistically significant (p-value ≤ 0.05) repolarization prolongation was first observed	Continuous
foldaym	Drug concentration (folds over C _{max}) when drug-induced arrhythmias were first observed	Continuous
pred7	Drug-induced repolarization change (ms) at C _{max}	Continuous

Table S2. The seven predictors in the stem cell dataset.

Predictor	Description	Type
c3v1	TdP score proposed in the original study ¹⁴	Continuous
c3v2	Interval between the J point and the start of T wave (JT)	Continuous
c3v3	Interval between the J point and the peak of T wave (JTP)	Continuous
c3v4	Ratio of the JTP interval at concentration ≥ 0 to concentration = 0	Continuous
c3v6	QS interval, measured at pace rate 2000	Continuous
c3v7	QS interval, measured at pace rate 500	Continuous
c3v8	Ratio of the QS interval at concentration ≥ 0 to concentration = 0, measured at pace rate 500	Continuous
c3v9	Interval between Q point and the end of T wave (QTE)	Continuous
c3v10	Ratio of the QTE interval at concentration ≥ 0 to concentration = 0	Continuous
c3v11	Ratio of QT interval to QS interval	Continuous
c3v12	Ratio of the interval between the peak and the end of T wave (TPE) to QT interval	Continuous
c3v13	Ratio of TPE interval ⁵² to QT interval	Continuous
c3v14	TPE Interval	Continuous
c3v15	Ratio of TPE interval at concentration ≥ 0 to concentration = 0	Continuous
c3v16	Score as a function of EAD ¹⁴	Continuous

Table S3. The 15 predictors in the wedge dataset. Except for extra notes, all predictors were obtained from an electrocardiogram at a 2000 pace rate.